

# Magnetic susceptibility in quasi one-dimensional $\text{Ba}_2\text{V}_3\text{O}_9$ : chain segmentation versus the staggered field effect

B. Schmidt,<sup>1,\*</sup> V. Yushankhai,<sup>1,2</sup> L. Siurakshina,<sup>3,2</sup> and P. Thalmeier<sup>1</sup>

<sup>1</sup>*Max Planck Institute for the Chemical Physics of Solids, Dresden, Germany*

<sup>2</sup>*Joint Institute for Nuclear Research, Dubna, Russia*

<sup>3</sup>*Max Planck Institute for the Physics of Complex Systems, Dresden, Germany*

A pronounced Curie-like upturn of the magnetic susceptibility  $\chi(T)$  of the quasi one-dimensional spin chain compound  $\text{Ba}_2\text{V}_3\text{O}_9$  has been found recently [1]. Frequently this is taken as a signature for a staggered field mechanism due to the presence of g-factor anisotropy and Dzyaloshinskii-Moriya interaction. We calculate this contribution within a realistic structure of vanadium  $3d$ - and oxygen  $2p$ -orbitals and conclude that this mechanism is far too small to explain experimental results. We propose that the Curie term is rather due to a segmentation of spin chains caused by broken magnetic bonds which leads to uncompensated  $S=\frac{1}{2}$  spins of segments with odd numbers of spins. Using the finite-temperature Lanczos method we calculate their effective moment and show that  $\sim 1\%$  of broken magnetic bonds is sufficient to reproduce the anomalous low- $T$  behavior of  $\chi(T)$  in  $\text{Ba}_2\text{V}_3\text{O}_9$ .

PACS numbers: 75.10.Jm, 75.40.Cx, 75.50.Ee

## I. INTRODUCTION

Recently a quasi one-dimensional magnetic behavior of  $\text{Ba}_2\text{V}_3\text{O}_9$  was clearly revealed by means of the magnetic susceptibility  $\chi(T)$  and the specific heat  $C_p(T)$  measurements in polycrystalline samples [1]. The data are compatible with the spin  $S = 1/2$  antiferromagnetic (AF) Heisenberg chain model with a nearest neighbor exchange coupling  $J = 94$  K. In addition an anomalous Curie-like upturn of  $\chi(T)$  was found below 20 K and claimed to be of intrinsic nature because the effect of paramagnetic impurities was ruled out by the analysis of experimental data. This low- $T$  behavior of  $\chi(T)$  was tentatively attributed in [1] to the staggered field effect induced by the applied magnetic field. In a quasi one-dimensional spin  $S = 1/2$  chain a low- $T$  upturn of  $\chi(T)$  is expected if the Dzyaloshinskii-Moriya (DM) interaction and/or a staggered  $g$ -factor anisotropy are present in the system [2, 3]. Among the  $3d$ -systems, Cu benzoate [4] and pyrimidine Cu dinitrate [5] are the most known examples. However the anomalous low- $T$  part of  $\chi(T)$  in Cu benzoate is much larger than in the theory [3] and the physical reason for this discrepancy is not yet clear. For better understanding, a comparative analysis of different sources contributing to the anomalous low- $T$  behavior of  $\chi(T)$  is necessary. In the present paper such an analysis is developed for  $\text{Ba}_2\text{V}_3\text{O}_9$  compound.

The low symmetry of  $\text{Ba}_2\text{V}_3\text{O}_9$  allows both a staggered  $g$ -factor anisotropy and a DM interaction to contribute to the staggered field. We suggest a simple model of vanadium  $3d$ - and oxygen  $2p$ -orbital structure within magnetic chains and calculate both contributions. Alternatively, we consider a segmented spin chain model where uncompensated spin moments lead to the low- $T$  Curie

term and compare the results of both models to the experimental  $\chi(T)$ . A segmented AF spin- $1/2$  chain model was applied earlier [6, 7] to explain the magnetic susceptibility measurements in quasi one-dimensional cuprates. In these studies, analytic results [6] and quantum Monte Carlo simulations [7] were used, assuming a particular random distribution of broken magnetic bonds (defects). Here we extend the segmented-chain model and compare different distributions of defects or chain segment lengths. To determine the thermodynamic properties of the chains under consideration, we apply the finite-temperature Lanczos method [8].

## II. ORBITAL STRUCTURE AND THE $g$ -TENSOR ANISOTROPY

According to [1]  $\text{VO}_6$  octahedra in  $\text{Ba}_2\text{V}_3\text{O}_9$  form edge-sharing chains. The  $\text{O}_6$  octahedron with an average V-O distance  $\simeq 2 \text{ \AA}$  is only slightly distorted, and  $\text{V}^{4+}$  ion ( $d^1$ -state) is displaced from the center by about  $0.2 \text{ \AA}$  towards one of the oxygens shared by two neighboring octahedra. The direction of V-ion off-center displacement distinguishes clearly a local  $z$ -axis in each  $\text{VO}_6$  octahedron. The energy splitting of vanadium  $d$ -orbitals was suggested [1] to be such that  $d_{xy}$ -orbital located in the plane transverse to the local  $z$ -axis is the singly occupied ground state orbital (Figure 1). Results of *ab initio* calculations of a small cluster confirm this picture. Within a chain the local  $z$ -axis varies in a zig-zag manner thus forming alternating short and long V-O bonds. The resulting  $d$ -orbital arrangement along a chain determines the symmetry and strength of a superexchange (SE) coupling between vanadium spins. Based on standard SE theory we calculate both the isotropic exchange constant  $J_{ij}$  and the DM vector  $\mathbf{D}_{ij}$  for neighboring V-ions.

First we calculate the  $g$  tensor components of the  $\text{V}^{4+}$  ion in the  $\text{VO}_6$  octahedron whose size is scaled to the one

\*Electronic address: bs@cpfs.mpg.de

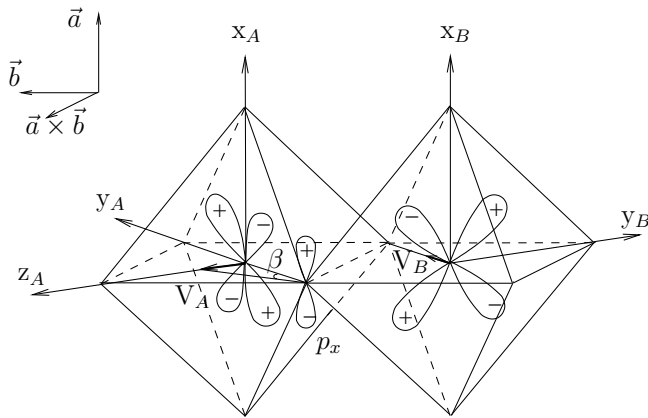


FIG. 1: Two edge-sharing  $\text{VO}_6$  octahedra forming a segment of a magnetic chain in  $\text{Ba}_2\text{V}_3\text{O}_9$ . The local coordinate systems attached to the A- and B-octahedra and the directions of the off-center displacements of the  $\text{V}_{A,B}$ -ions along the local  $z$ -axes are shown. The ground-state  $d_{xy}^A$  and  $d_{xy}^B$  orbitals of the  $\text{V}_{A,B}$ -ions and the relevant  $p_x$ -orbital of a common-edge oxygen ion responsible for the  $\text{V}_A$ - $\text{V}_B$  superexchange are shown. The  $d_{xy}$  orbitals in neighboring octahedra lie in orthogonal planes. The Dzyaloshinskii-Moriya vector  $\mathbf{D}_{AB}$  is parallel to  $\mathbf{a}$ -axis and alternates in sign on successive bonds.

in  $\text{Ba}_2\text{V}_3\text{O}_9$ . Strong variation of V-O covalent bonding due to a V-ion displacement from the central position in the nearly cubic  $\text{O}_6$  cage splits  $t_{2g}$  and  $e_g$  vanadium  $d$ -orbitals. We neglect the extra distortion of the crystal field on V-ions caused by the side ionic groups attached to the chains. Then the diagonal  $g$  tensor is given by  $g_{\parallel} = 2(1 - \Lambda_{zz})$ ,  $g_{\perp} = 2(1 - \Lambda_{\perp})$ , where  $\Lambda_{\perp} = \Lambda_{xx} = \Lambda_{yy}$ , and  $\Lambda_{\mu\mu} = \lambda \sum_{m \neq 0} |\langle 0 | L_{\mu} | m \rangle|^2 / (E_m - E_0)$ . Here,  $\lambda \simeq 0.03 \text{ eV}$  is the constant of spin-orbit coupling for  $\text{V}^{4+}$ -ions [9],  $L_{\mu}$  is the orbital angular momentum and  $|0\rangle$ ,  $|m\rangle$  are ground state and an excited  $d$ -orbital state respectively with an excitation energy  $E_m - E_0 \gg \lambda$ .

For a  $\text{VO}_6$  octahedron with one unpaired electron on vanadium  $d$ -shell we performed *ab initio* quantum chemical calculations of the ground state  $E_0$  and excited state  $E_m$  cluster energies as function of the  $\text{V}^{4+}$  ion displacement  $\delta$  along a local  $z$ -axis. The model cluster  $[\text{VO}_6]^{8-}$  was embedded in an octahedral point charge environment and the program package MOLPRO was used. First the restricted Hartree-Fock molecular orbital (MO) wave functions were determined to define an active space of MOs including a variety of valence and virtual orbitals (altogether 23 orbitals arising from strongly hybridized  $\text{V}(3d)$  and  $\text{O}(2p)$  states). Then the active space was used to take into account effects of electron correlations by performing multireference configurational interaction (MRCI) calculations of the cluster energies when the unpaired electron was placed successively in different  $d$ -orbitals. The results of these post Hartree-Fock calculations (Figure 2) show that  $t_{2g}$ -orbitals are split into the ground state orbital singlet  $|d_{xy}\rangle \equiv |0\rangle$  and degenerate orbital doublet  $|d_{xz}\rangle \equiv |1\rangle$ ,  $|d_{yz}\rangle \equiv |2\rangle$ . At the

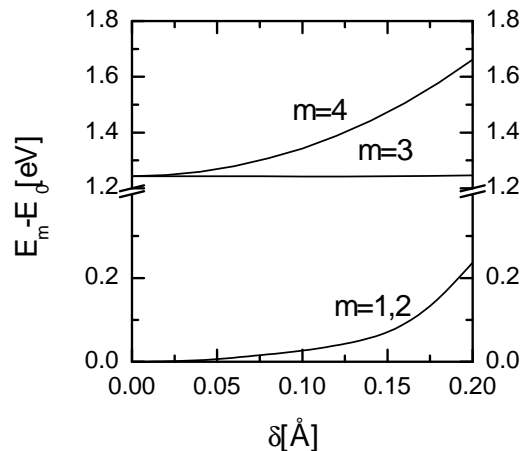


FIG. 2: Excitation energies  $E_m - E_0$  of the Vanadium  $3d$  states  $|m\rangle$  in  $\text{VO}_6$  as functions of the off-center displacement  $\delta$  of the  $\text{V}^{4+}$ -ion along the local octahedral  $z$ -axis.

physical displacement  $\delta = 0.2 \text{ \AA}$ , the energy difference between them is  $E_{1,2} - E_0 \simeq 0.23 \text{ eV} \equiv \Delta_1$ , while for  $|d_{x^2-y^2}\rangle \equiv |3\rangle$  one has  $E_3 - E_0 \simeq 1.26 \text{ eV} \equiv \Delta_3$ . Using  $\langle 1 | L_x | 0 \rangle = -\langle 2 | L_y | 0 \rangle = i$  and  $\langle 3 | L_z | 0 \rangle = -2i$  one obtains the following result for the  $g$ -factor anisotropy:  $(g_{\parallel} - g_{\perp}) \simeq 2\lambda(1/\Delta_1 - 4/\Delta_3) \simeq 0.07$ .

Next we define a global reference system with unit vectors  $\hat{\mathbf{x}} \parallel \mathbf{a}$ ,  $\hat{\mathbf{y}} \parallel \mathbf{b}$  and  $\hat{\mathbf{z}} \parallel \mathbf{a} \times \mathbf{b}$ , where  $\mathbf{a}$  and  $\mathbf{b}$  are orthogonal crystallographic axes in  $\text{Ba}_2\text{V}_3\text{O}_9$ . In this system the  $\hat{g}$  tensor is decomposed into a uniform  $\hat{g}_u$  and a staggered  $\hat{g}_s$  part,  $\hat{g}_\ell = \hat{g}_u + (-1)^\ell \hat{g}_s$ , where  $\ell$  denotes the V-sites along a chain. The only non-zero components of  $\hat{g}_s$  are  $(\hat{g}_s)_{yz} = (\hat{g}_s)_{zy} = g_s = (g_{\parallel} - g_{\perp}) \sin \alpha \cos \alpha$ , where  $\alpha$  is a tilt angle. In  $\text{Ba}_2\text{V}_3\text{O}_9$  the local  $z$ -axes are tilted from the chain direction ( $\mathbf{b}$ -axis) and  $\alpha \simeq 45^\circ$  alternates as  $\ell$  runs along the chain. Finally, our calculation leads to a staggered component  $g_s \simeq 0.035$  for  $\text{Ba}_2\text{V}_3\text{O}_9$ .

### III. ISOTROPIC EXCHANGE AND DZYALOSHINSKII-MORIYA INTERACTION

Considering now the intrachain magnetic coupling we note that for each (AB)-pair of neighboring V-ions the shortest SE path is via the out-of-plane  $p_x$ -orbital which belongs to one bridging oxygen as shown in Figure 1. To estimate the electronic hopping parameter  $t_{d\pi}$  of the  $\pi$ -bonding between each of occupied  $d_{xy}^{A,B}$ -orbitals and bridging oxygen  $p_x$ -orbital we use Harrison's prescription [10]:  $t_{d\pi} = \eta_{pd\pi} \hbar^2 r_d^{3/2} / (ma^{7/2})$ , where  $\eta_{pd\pi} = 1.36$ ,  $\hbar^2/m = 7.62 \text{ eV \AA}$  and  $r_d = 0.98 \text{ \AA}$  for vanadium. For the average V-O distance  $a \simeq 2 \text{ \AA}$  one obtains  $t_{d\pi} \simeq 1 \text{ eV}$ . Then from SE theory the isotropic exchange constant is obtained as

$$J \simeq \frac{4t_{d\pi}^4}{(U_d + \Delta_{d\pi})^2} \left[ \frac{1}{U_d} + \frac{2}{2(U_d + \Delta_{d\pi}) + U_\pi} \right], \quad (1)$$

where  $U_d$  and  $U_\pi$  are the on-site Coulomb integrals on V and O, respectively;  $\Delta_{d\pi} = \epsilon_d - \epsilon_\pi$  is the energy difference between the vanadium ground state  $d$ - and oxygen  $p_x$ -orbitals. We have  $\Delta_{d\pi} > 0$ , since  $\text{Ba}_2\text{V}_3\text{O}_9$  is a Mott-Hubbard insulator. We use the following parameter values (in eV):  $U_d = 3 \dots 4$ ,  $U_\pi = 2 \dots 6$ , and  $\Delta_{d\pi} \simeq 5$ , characteristic of vanadium oxides with tetravalent V-ions. This leads to an exchange  $J$  in the range  $10 \text{ meV} < J < 20 \text{ meV}$  in comparison to the experimental value  $J \approx 10 \text{ meV}$ . We conclude that the use of the shortest SE path via the common edge O-ion provides a satisfactory account of the isotropic AF exchange in  $\text{Ba}_2\text{V}_3\text{O}_9$ .

For a pair (AB) of V-ions the DM vector can be written [11] as  $\mathbf{D}_{AB} = -i(\mathbf{\Lambda}_A - \mathbf{\Lambda}_B)$  with  $\mathbf{\Lambda}_{A/B} = 2\lambda \sum_{m \neq 0} \langle m_{A/B} | \mathbf{L}_{A/B} | 0_{A/B} \rangle (E_m - E_0)^{-1} J_{A/B}^{(m)}$ . Here,  $J_A^{(m)} = J(m_A, 0_B; 0_A, 0_B)$  and  $J_B^{(m)} = J(0_A, m_B; 0_A, 0_B)$  are SE constants in similar intermediate configurations where the unpaired electron on the  $V_A$ - or  $V_B$ -ion, respectively, is raised by the spin-orbit interaction to  $m$ th excited  $d$ -state. The symmetry requires  $J(m_A, 0_B; 0_A, 0_B) = J(0_A, m_B; 0_A, 0_B) \equiv J_{AB}^{(m)}$ . In this notation, the isotropic constant calculated above reads  $J = 2J(0_A, 0_B; 0_A, 0_B) \equiv 2J_{AB}^{(0)}$ . For the orbital geometry in Figure 1, inspection shows that the only non-zero excited state exchange  $J_{AB}^{(m)}$  is for  $m = 1$ . This corresponds to the intermediate electronic configuration with occupied  $|d_{xz}\rangle$  state. The matrix elements of  $\mathbf{L}_A$  and  $\mathbf{L}_B$  are calculated by referring to a common coordinate system, which yields  $\langle 1_A | \mathbf{L}_A | 0_A \rangle - \langle 1_B | \mathbf{L}_B | 0_B \rangle = -2i\hat{\mathbf{e}}_{AB}$ , where the unit vector  $\hat{\mathbf{e}}_{AB}$  is defined as  $\hat{\mathbf{e}}_{AB} = \hat{\mathbf{z}}_A \times \hat{\mathbf{z}}_B$ . To compare  $J_{AB}^{(1)}$  and  $J_{AB}^{(0)}$ , we note that the hopping parameter  $t_{d\pi}^{(1)}$  between each of the excited vanadium  $d_{xz}^{A,B}$ -orbitals and the bridging oxygen  $p_x$ -orbital is related to  $t_{d\pi}$ -hopping as  $t_{d\pi}^{(1)} \simeq t_{d\pi} \sin \beta$ , where  $t_{d\pi}$  enters into the definition of  $J_{AB}^{(0)}$  and  $\sin \beta \simeq (\delta/a) \simeq 0.1$ . This immediately leads us to the simple result,  $J_{AB}^{(1)} \approx J_{AB}^{(0)} \sin \beta$ , hence  $\mathbf{D}_{AB}/J_{AB} = d \cdot \hat{\mathbf{e}}_{AB}$ , where  $d = (2\lambda/\Delta_1) \sin \beta \approx 0.025$ .

$\mathbf{D}_{AB}$  is staggered along the chain direction, i.e.  $\mathbf{D}_{\ell, \ell+1} = (-1)^\ell \mathbf{D}$  due to the property of  $\mathbf{e}_{\ell, \ell+1}$ . The geometric factor  $\sin \beta$  is a measure of the asymmetry caused by off-center displacements of V-ions. If they are neglected the inversion center at the midpoint of (AB)-pair is restored and  $\mathbf{D}_{AB} = 0$ .

#### IV. STAGGERED-FIELD MODEL FOR THE SUSCEPTIBILITY UPTURN IN $\text{Ba}_2\text{V}_3\text{O}_9$

Taking both effects described above into account, a magnetic field  $\mathbf{H}$  applied to a chain induces a staggered field  $\mathbf{h}$ , which can approximately be written [2, 3] as

$$\mathbf{h} \approx \frac{1}{J} \mathbf{D} \times \mathbf{H} + \hat{g}_s \mathbf{H}. \quad (2)$$

For  $T \ll J/k_B$ , the staggered field leads to a contribution to the magnetic susceptibility of the form [3]:

$$\chi_s(T) \simeq 0.2779c^2 \left( \frac{N_A \mu_0 \mu_B^2}{k_B} \right) \frac{\ln^{1/2}(J/k_B T)}{T}, \quad (3)$$

which scales with the factor  $c \sim h/H$ [2]. This should be compared with the experimental low- $T$  ( $2 \text{ K} < T < 20 \text{ K}$ ) behavior of  $\chi$  in  $\text{Ba}_2\text{V}_3\text{O}_9$  which is well described by a Curie law,  $\chi_{LT} = C_{LT}/T$ [1].

The staggered susceptibility  $\chi_s(T)$  varies approximately like  $C_s/T$ . For  $2 \text{ K} < T < 20 \text{ K}$ , we take into account the slowly varying logarithmic correction by replacing  $\ln^{1/2}(J/k_B T)$  with its average value  $\approx 1.6$ . Then, we obtain the Curie constant due to the staggered field as  $C_s \simeq 1.33c^2(N_A \mu_0 \mu_B^2/3k_B) = (N_A \mu_0/3k_B)(\mu_s^{\text{eff}})^2$ , where the second relation defines the effective staggered magnetic moment  $\mu_s^{\text{eff}} = \sqrt{1.33}c\mu_B$ .

In general the factor  $c^2$  is an angle dependent function of the magnetic field  $\mathbf{H}$  direction:  $c^2(\theta, \phi) = \sum_\mu (\partial h_\mu / \partial H_\alpha)^2$ ,  $\alpha = \alpha(\theta, \phi)$ . In a polycrystal used in [1], the angular average  $c^2 = \langle c^2(\theta, \phi) \rangle$  is measured. With  $\mathbf{D}$  and  $\hat{g}_s$  given, one obtains  $c^2 = (2/3)[d^2 + g_s^2]$ , yielding  $C_s \simeq 2.5 \cdot 10^{-3} \text{ cm}^3 \text{ K/mol}$ , and correspondingly an effective moment  $\mu_s^{\text{eff}} \simeq 4 \cdot 10^{-2} \mu_B$ .

In comparison the experimental values reported in [1], namely  $C_{LT} \simeq 6.0 \cdot 10^{-2} \text{ cm}^3 \text{ K/mol}$  and  $\mu_{LT}^{\text{eff}} \simeq 0.2 \mu_B$ , are much higher. Therefore we conclude that the staggered-field effect alone is not sufficient to explain the low-temperature behavior of the magnetic susceptibility in  $\text{Ba}_2\text{V}_3\text{O}_9$ , and a different mechanism must be present.

#### V. SEGMENTED-CHAIN MODEL FOR THE ANOMALOUS SUSCEPTIBILITY

The previous magnetic model implies a long-range order of short V-O bonds in each structural  $\text{VO}_2$ -chain. From Figure 1 we infer that several quasi-degenerate energy minima for the short V-O bonds orientation can exist. This expected structural degeneracy is described in an easy way by recalling that a local  $z$ -axis in each  $\text{VO}_6$  octahedron is defined in our description by the direction of the off-center V-ion displacement as is shown in Fig. 1. Then, for a separate chain, four degenerate ground state structural configurations correspond to the following decomposition of the local  $z$ -axes and their variation along a chain:  $\hat{\mathbf{z}}_\ell = \pm[\hat{\mathbf{b}} \cos \alpha \pm (-1)^\ell(\hat{\mathbf{a}} \times \hat{\mathbf{b}}) \sin \alpha]$ , with the tilt angle  $\alpha \simeq 45^\circ$ . Because of weak interchain interactions and the influence of the side ionic groups, the exact degeneracy can be partly removed. We suggest, however, that the remaining degeneracy can lead to a domain wall formation within a chain, which does not contradict the X-ray measurements reported in [1]. Chain segments with differently oriented bonds (domains) can spontaneously form at high temperatures during the growth and preparation of the sample. A chain domain wall with parallel neighboring local  $z_{A-}$  and  $z_{B-}$  axes corresponds to

the ground-state  $d_{xy}^A$  and  $d_{xy}^B$  orbitals that lie in parallel planes and thus have no short-parth SE connection. Therefore, the exchange interactions between end point spins of neighboring segments are strongly suppressed resulting in broken magnetic bonds which we call defects below.

Chain segmentation is an attractive possibility to explain the observed low-temperature Curie term in the magnetic susceptibility because segments with an odd number of spins lead to uncompensated  $S = 1/2$  states. In the following we calculate this contribution. The effective Hamiltonian used is the one-dimensional isotropic AF Heisenberg model,  $H = J \sum_{\ell} \mathbf{S}_{\ell} \mathbf{S}_{\ell+1}$ , and we ignore the staggered-field terms discussed before in the following analysis.

For the joint probability of having no defect between positions 0 and  $x$ , but one defect at position  $x$  on a particular chain, or the probability to find a spin chain of length  $x$ , we use a generalized Poisson distribution of the form

$$P(x) = f(x) \exp\left(-\int_0^x f(t) dt\right). \quad (4)$$

Here,  $f(x)$  describes the differential probability to find a defect at the distance  $x$  measured from a defect located at the origin. For the standard Poisson distribution,  $f(x) = 1/\rho$  is just a constant, i. e., is independent from the distance to the origin.

A Poissonian distribution of chain lengths overemphasizes the number of short chains. Instead, we expect that their fraction is small and the distribution peaks at a finite value because defects which are close by “repel” each other due to their larger elastic energies. Lacking a detailed microscopic model for this mechanism, we simply assume that the probability of defects at a distance  $x$  grows linearly with  $x$  like  $f(x) = \frac{\pi}{2}\rho^2 x$ , leading to

$$P(x) = \frac{\pi}{2}\rho^2 x \exp\left(-\frac{\pi}{4}\rho^2 x^2\right). \quad (5)$$

Here,  $\rho$  is the number of broken bonds per unit length of an infinite chain, i. e., the inverse average chain length. This is the Wigner distribution, well-known from quantum statistics.

## VI. NUMERICAL PROCEDURE AND RESULTS

We use the finite-temperature Lanczos method [8] to calculate the eigenvalues, eigenvectors, and thermodynamic properties for the segmented chains. To comply with the effect of broken bonds, we use open boundary conditions. Then the only symmetries remaining to reduce the size of the problem are  $[H, \mathbf{S}^2] = 0$  and  $[H, S_z] = 0$ . While the latter can be implemented easily using an appropriate basis, there is no simple way to efficiently incorporate the former. To compute finite-temperature expectation values, we have to store *all* calculated Lanczos eigenvalues and *all* of the corresponding

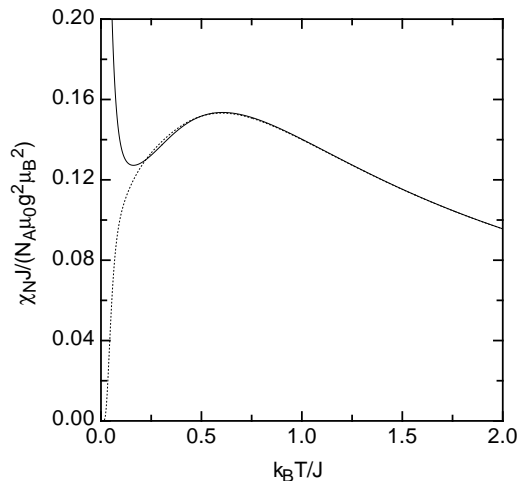


FIG. 3: Temperature dependence of the uniform magnetic susceptibility of Heisenberg chains of length 23 (solid line) and 24 (dotted line) with open boundary conditions.

eigenvector coefficients in terms of the basis, which is the limiting computational requirement here, in contrast to ground-state calculations.

We have calculated the uniform magnetic susceptibility  $\chi_N$  for Heisenberg chains with length  $N$  between two and 24 sites, defined by

$$\chi_N(T) = \frac{N_A \mu_0 g^2 \mu_B^2}{N k_B T} \left( \langle (S_z^{\text{tot}})^2 \rangle - \langle S_z^{\text{tot}} \rangle^2 \right), \quad (6)$$

where  $\langle \dots \rangle$  denotes the thermal average,  $N_A$  is the Avogadro constant,  $\mu_0$  the magnetic permeability,  $g$  the gyromagnetic ratio,  $\mu_B$  the Bohr magneton, and  $k_B$  the Boltzmann constant. For the present nonmagnetic system  $\langle S_z^{\text{tot}} \rangle = 0$ .

To illustrate the results, Figure 3 shows the temperature dependence of the magnetic susceptibility for chains of length 23 and 24. According to Bonner and Fisher [12], the maximum of the susceptibility for an infinite Heisenberg chain is given by  $\chi_{\infty}^{\text{max}} J / (N_A \mu_0 g^2 \mu_B^2) \approx 0.147$  and is reached at a temperature of  $k_B T_{\text{max}} / J \approx 0.641$ . For the 24-site chain, the corresponding results are 0.153 for the maximum susceptibility, and 0.601 for the position of the maximum.

From the low-temperature upturn of  $\chi_N$  ( $N$  odd), we have extracted the effective moment  $\mu_{\text{eff}}(N)$  for each value of  $N$ . These data are shown in Figure 4 as the open squares. The effective moments as a function of the inverse chain length scale perfectly according to  $\mu_{\text{eff}}(N) = \sqrt{3/N} \mu_B$ . The factor  $\sqrt{3}$  originates from the definition of the effective moment via Curie’s law,  $\chi_C = N_A \mu_0 \mu_{\text{eff}}^2 / (3 k_B T)$ .

The effective moment as a function of the mean chain length  $N$  after averaging over chains of different size (even and odd) is shown in Figure 3 as open circles, representing the Wigner distribution and diamonds, representing the Poisson distribution. Data are shown for

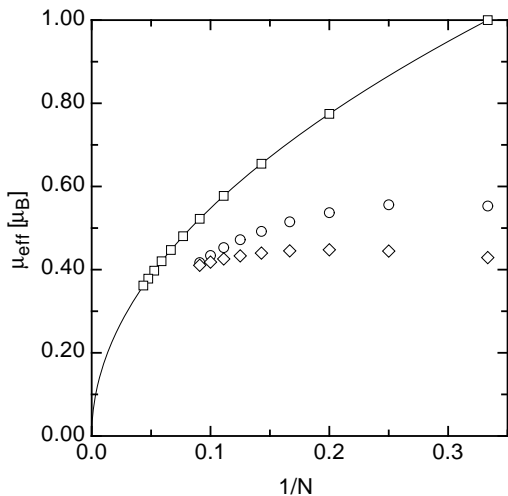


FIG. 4: Calculated effective moments in units of the Bohr magneton as a function of the inverse chain length. Squares denote the results for chains of a single fixed length, circles for the Wigner average, diamonds for the Poisson average with mean  $N$  over chain lengths between two and 24. The line denotes the dependence  $\mu_{\text{eff}}(N) = \sqrt{3/N} \mu_B$ .

$N \leq 11$ , because for a larger mean length, the chains of size greater than 24 would contribute significantly to the average susceptibility.

The main effect for both averages is to reduce the magnetic moment for short mean chain lengths. For the Wigner distribution, this is due to the linear suppression of the weight of the susceptibilities for the shortest chains, whereas for the Poisson distribution, the moment reduction is due to a comparatively large weight of the longer chains in the partition sum. Independent of how the average is performed, the effective moment is reduced because chains with an even site number, and thus no Curie term at low  $T$ , are also included in the average. The data suggest that for mean chain lengths  $N$  larger than 10, the average effective moment depends only weakly on the details of defect distribution.

In Figure 5, the experimental data for the susceptibility  $\chi$  of  $\text{Ba}_2\text{V}_3\text{O}_9$  are plotted as  $\chi \cdot T$  versus temperature  $T$ . A fit to these between  $T = 2$  K and 10 K of the form  $\chi = C/T + \chi_{\text{VV}}$  with  $C = N_A \mu_0 \mu_{\text{eff}}^2 / (3k_B)$  yields an average moment of  $\mu_{\text{eff}} \approx 0.2 \mu_B$ . A mean chain length of the order of 75 spins would be necessary to explain the experimentally observed Curie upturn by the segmentation of  $\text{VO}_2$  chains.

## VII. CONCLUSION

We have discussed two alternative models for the anomalous Curie term in the low- $T$  susceptibility of

$\text{Ba}_2\text{V}_3\text{O}_9$ . We find that within our approximate calculation the staggered field mechanism is far too small to explain the observed effective moment. Therefore we

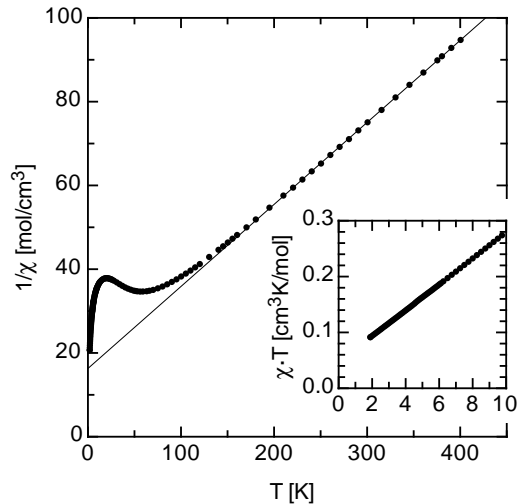


FIG. 5: Curie plot of the susceptibility of  $\text{Ba}_2\text{V}_3\text{O}_9$ . The straight line illustrates a fit of the form  $\chi = C_0/(T + \Theta_{\text{CW}})$  for temperatures  $T$  between 200 K and 400 K. In the inset, the same data are plotted as susceptibility times temperature versus  $T$  for low temperatures.

propose a different mechanism for the Curie term which is based on chain segmentation due to broken magnetic bonds which leads to uncompensated effective moments on segments with odd number of spins. We find that a rather low concentration of  $\sim 10^{-2}$  broken bonds can explain the observed Curie term. A definite distinction between the two models requires the investigation of the field-orientation dependence of the susceptibility in monocrystals of  $\text{Ba}_2\text{V}_3\text{O}_9$ .

## Acknowledgments

We wish to thank Henk Eskes for supplying his exact-diagonalization routines which were included in the finite-temperature Lanczos code used here. We thank Enrique Kaul for discussions and for supplying his experimental data.

- 
- [1] E. E. Kaul, H. Rosner, J. Sichelschmidt, R. V. Shpanchenko, C. Geibel, and V. Yushankhai, cond-mat/0209409, submitted to Phys. Rev. B.
- [2] M. Oshikawa and I. Affleck, Phys. Rev. Lett. **79**, 2883 (1997).
- [3] I. Affleck and M. Oshikawa, Phys. Rev. B **60**, 1038 (1999).
- [4] D. C. Dender, D. Davidović, D. H. Reich, and C. Broholm, Phys. Rev. B **53**, 2583 (1996).
- [5] R. Feyerherm, S. Abens, D. Günther, T. Ishida, M. Meißner, M. Meschke, T. Nogami, and M. Steiner, J. Phys.: Condens. Matter **12**, 8495 (2000).
- [6] H. Asakawa, M. Matsuda, K. Minami, H. Yamazaki, and K. Katsumata, Phys. Rev. B **57**, 8285 (1998).
- [7] V. Kiryukhin, Y. J. Kim, K. J. Thomas, F. C. Chou, R. W. Erwin, Q. Huang, M. A. Kastner, and R. J. Birgeneau, Phys. Rev. B **63**, 144418 (2001).
- [8] J. Jaklic and P. Prelovsek, Advances in Physics **49**, 1 (2000).
- [9] A. Abragam and B. Bleaney, *Electron paramagnetic resonance of transition ions* (Dover Publications, Inc., New York, 1970).
- [10] W. A. Harrison, *Electronic Structure and the Properties of Solids* (Dover Publications, Inc., New York, 1989).
- [11] F. Keffer, Phys. Rev. **126**, 896 (1962).
- [12] J. C. Bonner and M. E. Fisher, Phys. Rev. **135**, A640 (1964).